

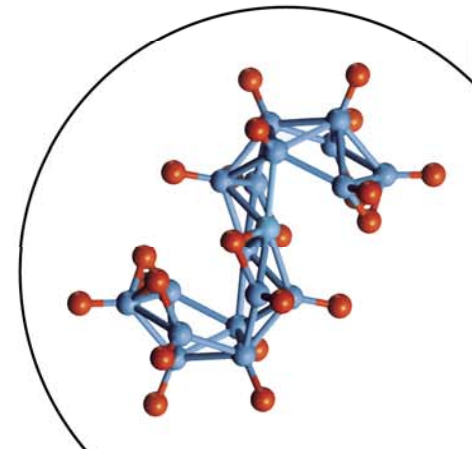


The Cluster Implant Source

Universal Cluster Source

Thomas N. Horsky, Sami K. Hahto, Edward K.
McIntyre, and George P. Sacco, Jr. / June 8, 2010

IIT 2010, Kyoto, Japan



Abstract

- We describe our newest Clusterlon[®] source, and show detailed data for $B_{18}H_x^+$, $C_7H_7^+$, $C_{16}H_x^+$, P_4^+ , and As_4^+ beams. These species are derived from both low-temperature solids and gaseous sources.
- 2D beam profiles are presented, along with mass spectra, beam current performance, and long-term beam reproducibility.
- The data were collected using the injection stage of a commercial ion implanter equipped with a 120 degree analyzer magnet. Beam profiles at magnet entrance and exit planes were produced using a specially designed 2D profiler.
- Beam currents were measured after mass analysis using a Faraday cup over an effective energy range of 200 eV to 10 keV.

Introduction

- Molecular or cluster implantation has become an important tool for shallow P+ doping of PMOS transistors. It is now well established [1,2] that the increased amorphization achieved with molecular ions not only improves activation, but results in devices with reduced transistor leakage [3,4].
- More recently, significant interest has emerged in using carbon clusters to incorporate strain into the NMOS S/D region. In addition, phosphorus has replaced arsenic as the dopant of choice in certain leading edge devices owing to the increased activation of phosphorus possible with modern annealing techniques.

Introduction (continued)

- This has led to the use of multiple molecular implant species to create certain portions of the transistor, for example, the PMOS S/D extension (boron doping and carbon diffusion control implants) and the NMOS S/D (carbon for strain, and phosphorus or arsenic for S/D and extension doping).
- Therefore, there is currently a need for molecular ion beams of not only boron-containing species, but also for n-type dopants and carbon, in order to enable improved device characteristics. To fill this need, SemEquip® has developed an ion source and ion optics to produce intense beams of molecular and cluster ions which are compatible with all conventional, beam line-based ion implantation systems.

Injector Test Stand

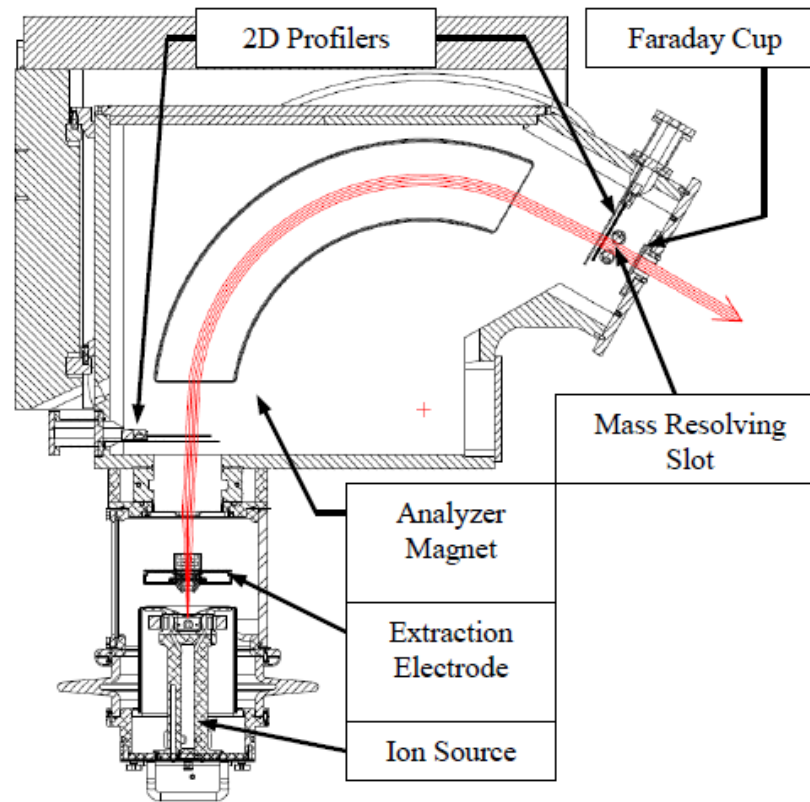


FIGURE 1. 2D schematic of the injector test stand, showing the basic hardware and diagnostic elements.

Ion Source

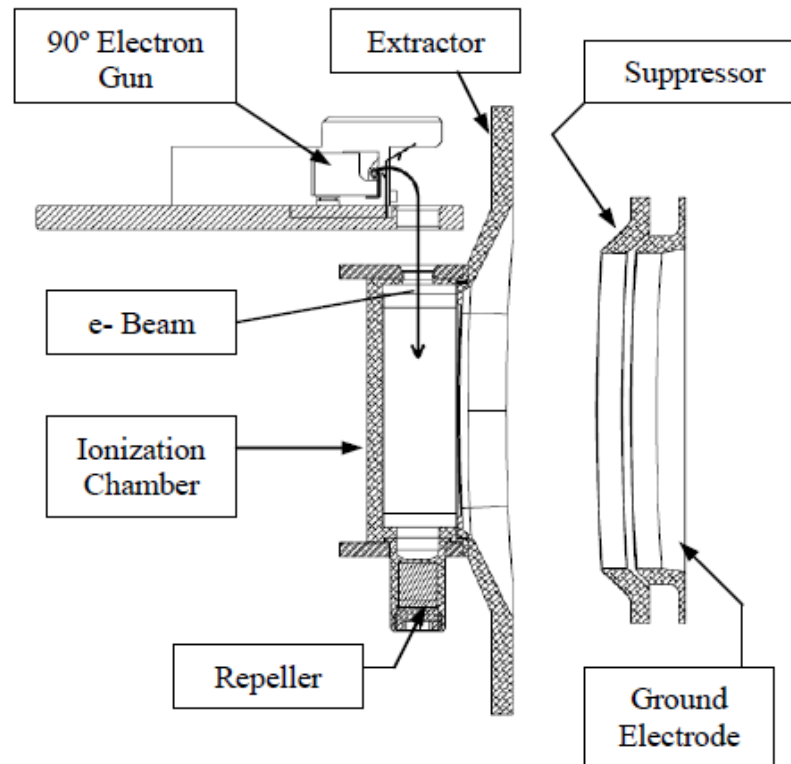


FIGURE 2. Ion Source and extraction electrode schematic.

Ion Source Description

- Figure 2 shows a schematic diagram of the ion source and extraction optics [6]. The ion source incorporates a 90 degree, magnetically focused electron gun located external to the ionization chamber in order to increase source reliability and extend filament lifetime.
- An intense electron beam is directed into the chamber, creating ions adjacent to the source extraction slot, where they are extracted and focused by the electric field between the extractor and suppressor electrodes.
- The electron beam is confined by a uniform magnetic field transverse to the direction of beam propagation. The ionization efficiency is further increased by a repeller, which acts to increase the effective path length of the primary electrons.

Vapor Delivery System

- Vapors of $B_{18}H_{22}$, $C_{16}H_{10}$, and $C_{14}H_{14}$ were introduced into the ion source using a commercial vapor delivery system (VDS) designed by SemEquip which has been previously described [7].
- Sealed vaporizer canisters containing 200g each of high purity material were used. The vaporizers interface directly to the temperature-controlled VDS which feeds a constant flow of vapor to the ion source through closed-loop control.
- In this study, vapor flow matched set point values to within less than 1%.

Solid Feed Materials: $C_{14}H_{14}$, $C_{16}H_{10}$, $B_{18}H_{22}$

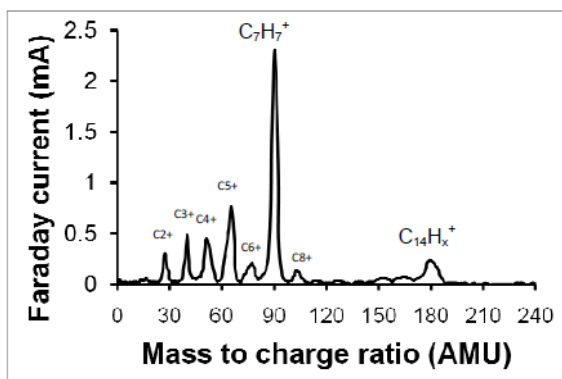


FIGURE 3. Mass analysis scan of a 20 kV $C_{14}H_{14}$ beam measured at the MRS Faraday.

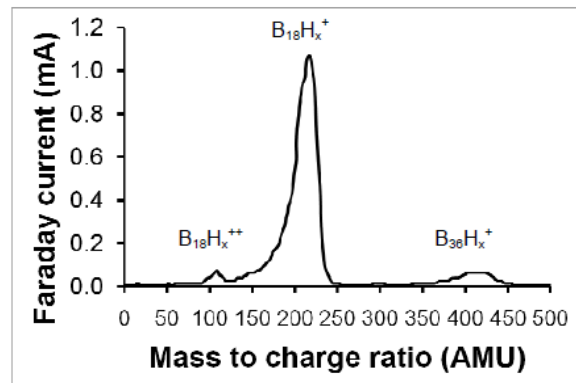


FIGURE 5. Mass analysis scan of a 20 kV $B_{18}H_{22}$ beam measured at the MRS Faraday.

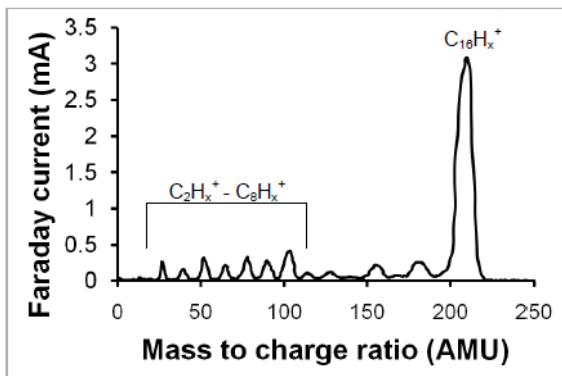


FIGURE 4. Mass analysis scan of a 20 kV $C_{16}H_{10}$ beam measured at the MRS Faraday.

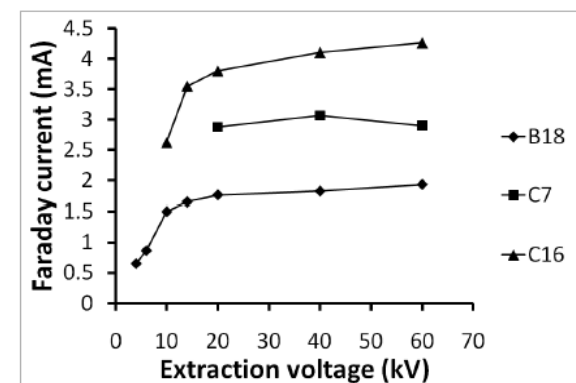


FIGURE 6. Extraction voltage dependence of mass analyzed $B_{18}H_x^+$, $C_7H_7^+$, and $C_{16}H_x^+$ beams.

2D Beam Profiles: $C_{14}H_{14}$, $B_{18}H_{22}$

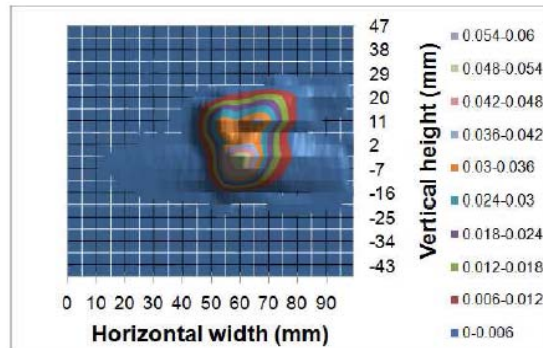


FIGURE 7. 20 keV 2D beam profile of $C_{14}H_{14}$ at the entrance to the mass analysis magnet. Beam intensity is shown as a 2D contour map. FWHM is 19 mm; FHHM is 24 mm.

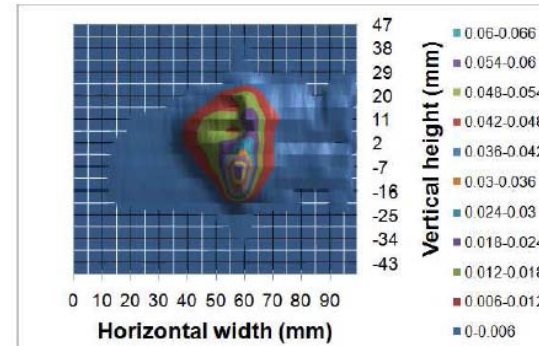


FIGURE 9. 20 keV 2D beam profile of $B_{18}H_{22}$ at the entrance to the mass analysis magnet. Beam intensity is shown as a 2D contour map. FWHM is 11 mm; FHHM is 18 mm.

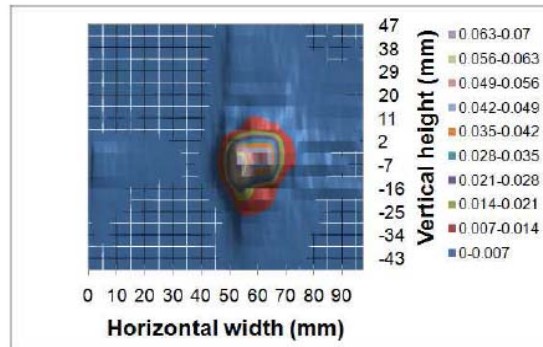


FIGURE 8. 20 keV 2D beam profile of $C_{14}H_{14}$ at the exit of the mass analysis magnet. Beam intensity is shown as a 2D contour map. FWHM is 16 mm; FHHM is 16 mm.

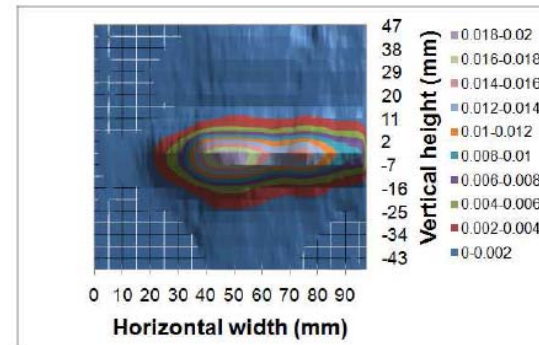


FIGURE 10. 20 keV 2D beam profile of $B_{18}H_{22}$ at the exit of the mass analysis magnet. Beam FWHM is 31 mm and FHHM is 15 mm over a 20 AMU-wide mass distribution centered on the $B_{18}H_x^+$ peak at 210 AMU.

Gaseous Materials: AsH_3 , PH_3

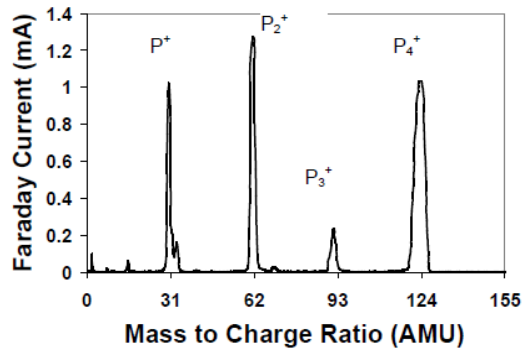


FIGURE 12. Mass analysis scan of a 20 kV PH_3 beam measured at the MRS Faraday.

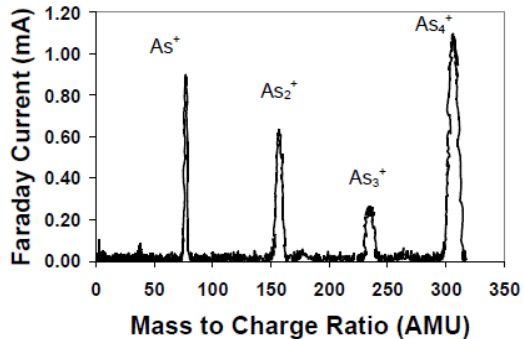


FIGURE 13. Mass analysis scan of a 20 kV AsH_3 beam measured at the MRS Faraday.

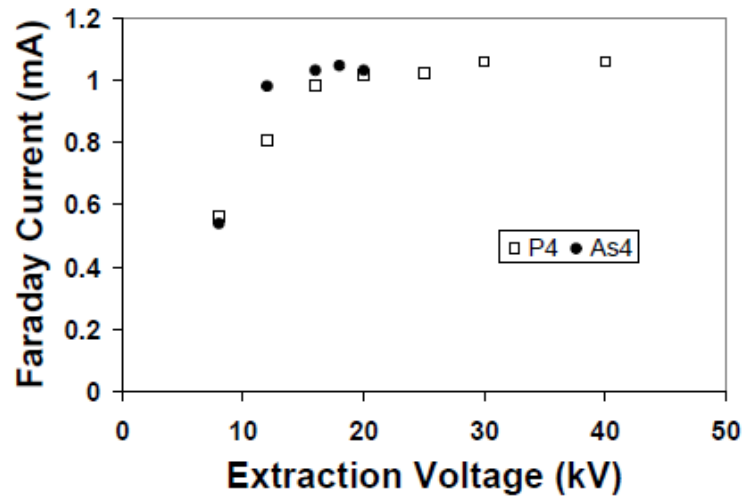


FIGURE 14. Extraction voltage dependence of mass analyzed P_4^+ and As_4^+ beams.

Beam Stability: $B_{18}H_x^+$, P_4^+ , As_4^+

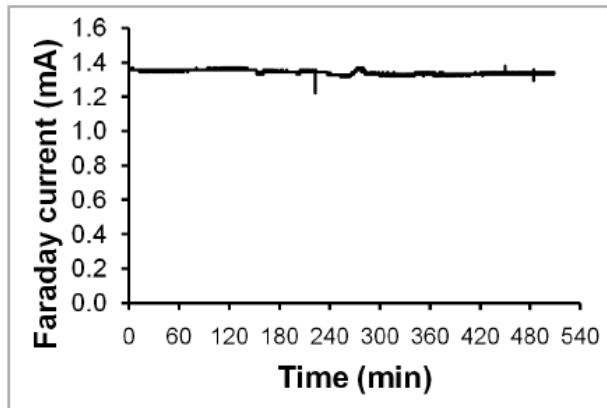


FIGURE 11. Beam current stability for a 20 keV $B_{18}H_x^+$ beam. No source tuning or other intervention was performed.

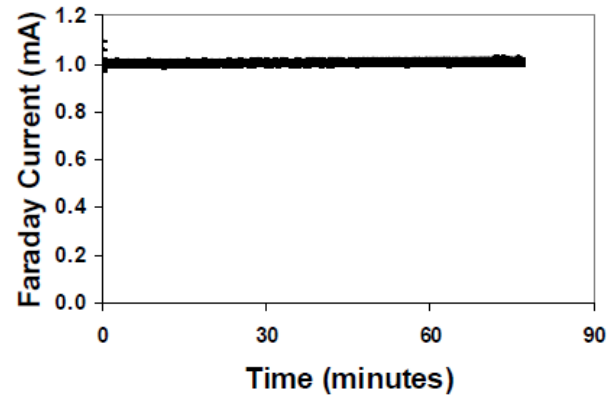


FIGURE 15. Beam current stability for a 20 keV P_4^+ beam. No source tuning or other intervention was performed.

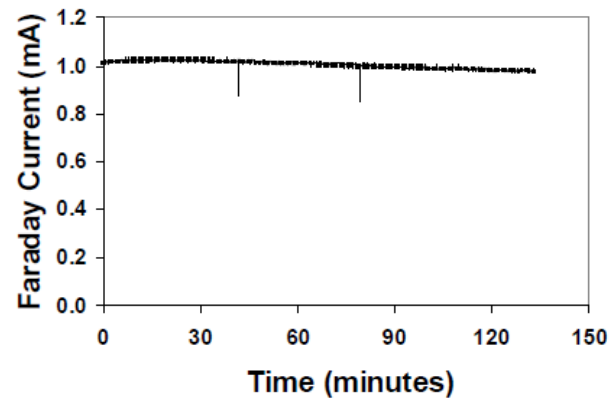


FIGURE 16. Beam current stability for a 20 keV As_4^+ beam. No source tuning or other intervention was performed.

Summary

- The ClusterIon[®] source and its beam injection system have been characterized with respect to beam current performance over a range of beam energies, from 4 keV to 60 keV, for the ion species $B_{18}H_x^+$, $C_7H_7^+$, $C_{16}H_x^+$, P_4^+ , and As_4^+ .
- 2D beam profiles were collected for $C_{14}H_{14}$ and $B_{18}H_{22}$ feed gases, and long-term beam stability was measured for $B_{18}H_x^+$, P_4^+ , and As_{4+} beams.
- The injector system demonstrated equivalent C monomer current of up to 67 mA, equivalent B current of up to 27 mA, and equivalent P and As currents of 4 mA.
- Beam current stability and reproducibility were excellent.

References

1. K. Uejima *et al.*, IEDM 2007, Sept 8, 2007
2. K. Yako *et al.*, JSAP 2007, Sept 8, 2007
3. F. Ootsuka *et al.*, IEEE Trans. Electron Dev. 55 (4), April, 2008
4. Y. Kawasaki *et al.*, IIT 2008, Monterey, CA, June 8, 2008
5. M. Tanjyo *et al.*, IWJT 2010, May 10-11, 2010, Shanghai, PRC
6. T. N. Horsky *et al.*, IIT 2006, June 11. 2006, Marseilles, France, pp. 198-201
7. D. Adams *et al.*, *ibid*, pp. 178-181
8. M. Tanjyo *et al.*, 8th Workshop on Cluster Ion Beam Technology, Tokyo, Japan, Nov. 8, 2007